THE JOURNAL OF PHYSICAL CHEMISTRY B

Article

pubs.acs.org/JPCB

Hydration Dynamics of a Halophilic Protein in Folded and Unfolded States

Johan Qvist,[†] Gabriel Ortega,[‡] Xavier Tadeo,[‡] Oscar Millet,[‡] and Bertil Halle*[,†]

[†]Department of Biophysical Chemistry, Center for Molecular Protein Science, Lund University, SE-22100 Lund, Sweden

[‡]Structural Biology Unit, CIC bioGUNE, Derio, Spain

Supporting Information

ABSTRACT: Proteins from halophilic microorganisms thriving at high salinity have an excess of charged carboxylate groups, and it is widely believed that this gives rise to an exceptionally strong hydration that stabilizes these proteins against unfolding and aggregation. Here, we examine this hypothesis by characterizing the hydration dynamics of a halophilic model protein with frequency- and temperature-dependent ^{17}O magnetic relaxation. The halophilic protein Kx6E was constructed by replacing six lysine residues with glutamate residues in the IgG binding domain of protein L. We also studied the unfolded form of Kx6E in the absence of salt. We find that the hydration dynamics of Kx6E does not differ from protein L or from other previously studied mesophilic proteins. This finding challenges the hypothesis of exceptional hydration for halophilic proteins. The unfolded form of Kx6E is found to be expanded, with a weaker dynamical perturbation of the hydration water than for folded proteins.

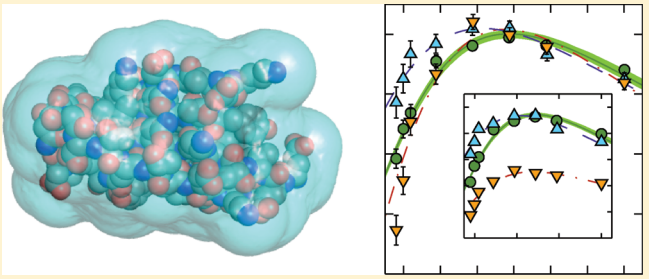

INTRODUCTION

Extreme halophilic archaea avoid osmotic dehydration by maintaining a high intracellular ion concentration (up to 4 M). Whereas mesophilic proteins tend to unfold and/or aggregate under such conditions, halophilic proteins not only tolerate but also are actually stabilized by high salinity. Indeed, many halophilic proteins unfold when the salt concentration is reduced. Several molecular mechanisms have been proposed to rationalize this unusual behavior.[1−4]

Halophilic proteins differ from their mesophilic counterparts most conspicuously in being more acidic.[1,5,6] In particular, aspartate is more and lysine less abundant, resulting in a large negative net charge at neutral pH. In addition, bulky hydrophobic side chains are less prevalent in halophilic proteins.[7] The enhanced net surface charge density of halophilic proteins might seem to explain their solubility at high salinity and their reduced stability at lower salinity, but screened Coulomb interactions cannot be the whole story.[1,8] At salt concentrations of several molar, most water molecules in the solvent are directly coordinated to inorganic ions. Significant salt effects are therefore expected on *all* solvent-averaged effective interactions, including Coulomb interactions (lower dielectric constant[8]), hydrogen bonds, and solvation of polar as well as apolar groups (enhanced hydrophobic effect[9]).

A recurring theme in the search for the molecular determinants of halo-adaptation has been the notion that halophilic proteins, on account of their high surface density of negatively charged aspartate and glutamate side-chains, are more strongly hydrated than other proteins.[3,4,10−16] Model-dependent interpretations of thermodynamic observables have suggested that halophilic proteins "bind" or are "associated" with a larger number of water molecules than mesophilic proteins. It is often argued[3,10,11,14] that this view is consistent with the finding, from proton NMR intensity measurements on partly frozen polypeptide solutions, that aspartate and glutamate are associated with more unfrozen water than are other amino acid side chains.[17] Moreover, the extensive hydration inferred from these studies is widely believed to protect halophilic proteins against unfolding and aggregation at high salinity.

A "solvation-stabilization model" has been proposed, according to which specific arrangements of carboxylate groups on the halophilic protein surface nucleate cooperative networks of water molecules and ions.[3,13] High-resolution crystal structures of halophilic proteins[14−16] have failed to identify such networks, and the few monovalent cations that have been localized tend to coordinate backbone carbonyl oxygens rather than carboxylates.[15,16] Nevertheless, the 1.9 Å crystal structure of halophilic ferredoxin was taken to support the notion of exceptional hydration of halophilic proteins, with an "immobile", "quasi-crystalline" first layer of "tightly bound" water molecules inducing an additional four organized water layers.[4,15] Similarly, the 1.6 Å crystal structure of halophilic glucose dehydrogenase revealed a "highly ordered, multilayered solvation shell", and the "stability" of this shell was linked to the low abundance of flexible side chains (notably, lysine) on the surface of halophilic protein.[16]

Received: January 3, 2012
Revised: February 9, 2012
Published: February 13, 2012

Quasielastic neutron scattering measurements on intact cells have been taken as evidence for a 250-fold mobility reduction for most of the cytoplasmic water in the extreme halophile *Haloarcula marismortui*, whereas little or no slowing down of cell water was evident for *Escherichia coli*.[18] It was suggested that the dramatic mobility reduction in the halophile is linked to "water bound to the halophile carboxyl-salt ion structures",[19] presumably the same structures that are postulated in the "solvation-stabilization model".[3,13]

To shed further light on the hydration properties of halophilic proteins, we have measured the ^{17}O nuclear spin relaxation rate of water molecules in aqueous solutions of the immunoglobulin G binding B1 domain of protein L (ProtL) from *Streptococcus magnus*[20,21] and a mutant form (Kx6E), where six lysines (residues 23, 28, 41, 42, 54, and 61) on the protein surface have been replaced by glutamates.[7] Protein L has been thoroughly characterized with respect to folding and stability,[22,23] including the effect of salts.[24,25] The large number of carboxylate groups (17) and the large negative net charge (−15 at neutral pH) of the Kx6E mutant (64 residues) are nearly the same as for *Haloarcula marismortui* ferredoxin (128 residues)[15] when adjusted for the 2-fold size difference. As for naturally occurring halophilic proteins, the stability of the Kx6E mutant increases with salinity, and the protein unfolds in the absence of salt.[7] The mutant Kx6E and the parent protein ProtL can therefore serve as a model halophilic−mesophilic pair.

Oxygen-17 spin relaxation monitors water molecules selectively (without complications from labile hydrogens) and reports on the single-molecule rotational correlation time (without complications from cross-correlations and intermolecular couplings).[26,27] By recording the longitudinal spin relaxation rate, R_1, as a function of resonance frequency—the magnetic relaxation dispersion (MRD) profile—we obtain information about long-lived internal water molecules as well as about the more mobile water molecules interacting with the external protein surface.[26−28] To characterize the surface hydration in more detail, we measured R_1 at high frequency (where internal water molecules do not contribute) over a wide temperature range extending into the supercooled regime.[29] Freezing of the solvent was prevented by dispersing the protein solution in micrometer-sized emulsion droplets that are large enough that the oil−water interface has negligible effect on water dynamics but small enough to allow supercooling to near the homogeneous nucleation temperature.[30] Here we report the ^{17}O MRD profile and the temperature dependence of R_1 over a 60 K interval for ProtL and for the Kx6E mutant with and without salt.

A second objective of this study is to characterize the hydration dynamics of the unfolded state of the Kx6E mutant in the absence of salt. Even though the protein−solvent interaction (in particular, the hydrophobic effect) is widely regarded as the principal driving force for protein folding,[31] unambiguous information about the properties of hydration water in unfolded proteins is still scarce. The ^{17}O MRD technique has been used to study proteins denatured by heat,[32] cold,[33] pH,[34] urea,[33,35] and guanidinium chloride,[34] but the interpretation is complicated by nonphysiological conditions, by protein aggregation, and, in the latter two cases, by denaturant binding.[28] The Kx6E mutant offers a unique possibility to study an unfolded protein under ambient conditions without external destabilizing perturbations.

MATERIALS AND METHODS

Sample Preparation. The wild-type and Kx6E mutant of the immunoglobulin G binding B1 domain of protein L from *Streptococcus magnus* (ProtL) were cloned, expressed, and purified as described.[7,25] The proteins were dissolved in water enriched to 21% in ^{17}O (Isotec). Kx6E solutions were prepared without added salt and with 750 mM NaCl (>99.5%, Merck). The protein solutions also contained phosphate buffer (19 mM for ProtL and 7 mM for Kx6E) and 2 mM NaN_3, and pH was adjusted to 7.8 ± 0.1 with NaOH and HCl. Three solvent reference samples were prepared with the same solvent composition as in the corresponding protein solutions. The final protein concentrations were determined from the absorbance at 280 nm in the presence of 4−5 M guanidinium chloride, using an extinction coefficient of 9757 mol^{-1} cm^{-1} (2% below the theoretically estimated value) based on a complete amino acid analysis of the ProtL sample. For relaxation measurements at subzero temperatures, the protein and reference solutions were confined in micrometer-sized emulsion droplets as described.[29,33]

Control Experiments. To assess protein secondary structure, circular dichroism spectra were recorded in the far-UV region 205−260 nm using a Jasco J-815 CD spectropolarimeter equipped with a PTC-423S Peltier effect cell holder. The CD spectra were acquired at 300 K with protein concentrations in the micromolar range (from NMR samples diluted with the corresponding buffer) and a path length of 1.0 cm. The reported data are averages of four spectra, recorded with a scan rate of 1 nm s^{-1}.

The fraction of unfolded protein was estimated from one-dimensional ^1H NMR spectra, recorded at 300 K on the samples that were also used for ^{17}O relaxation measurements. The ^1H spectra were acquired on a Varian Unity Plus 600 spectrometer using Watergate 3919 water suppression, four transients, and no frequency lock (to avoid adding D_2O to the solvent).

To rule out protein aggregation, water ^1H MRD profiles were recorded at 300 K in the frequency range 10 kHz−40 MHz using a Stelar Spinmaster 1T fast field cycling instrument. This technique can detect even very small populations of protein aggregates,[36] but none were seen in the samples used for ^{17}O relaxation measurements.

To detect any effects of the emulsion droplet interface, ^{17}O relaxation measurements were carried out at 300 K on all three protein solutions before and after incorporation into emulsion droplets. No significant difference in R_1 was detected between the original solutions and the corresponding emulsified samples.

^{17}O Magnetic Relaxation Dispersion Measurements. The dispersion of the water ^{17}O longitudinal relaxation rate R_1 was measured at 27.1, 67.8, and 81.3 MHz with the aid of fixed-field superconducting magnets (Bruker Avance 200, Varian Unity Plus 500 and 600) and in the frequency range 2.1−11.5 MHz with a field-variable resistive magnet (Drusch) interfaced to a Tecmag Discovery console. The sample temperature was maintained at 300.2 ± 0.1 K with a regulated flow of dried air and was measured before and after each relaxation measurement with a copper-constantan thermocouple referenced to an ice−water bath. At each field, R_1 was measured for a protein sample and then for the corresponding reference sample, using the inversion recovery method with 30−40 relaxation delays and a sufficient number of transients to obtain a signal-to-noise

dx.doi.org/10.1021/jp3000569 | J. Phys. Chem. B 2012, 116, 3436−3444

ratio larger than 100. On the basis of repeated measurements, the accuracy in R_1 was estimated to 1.0% at the two lowest frequencies and 0.5% at all other frequencies.

Temperature-Dependent R_1 Measurements. For the emulsified samples, the water ^{17}O longitudinal relaxation rate R_1 was measured at 81.3 MHz on a Varian Unity Plus 600 spectrometer as described above, except that the precooled air used for temperature regulation was subjected to an extra drying step. During thermal equilibration (at least 20 min, but up to 40 min at the lowest temperatures), R_1 was measured repeatedly to ensure that temperature oscillations had been damped out and that stable R_1 values were obtained. At sufficiently low temperatures, where a significant fraction of the emulsion droplets freeze by homogeneous nucleation (as seen by a reduction of the integrated ^{17}O peak area), the released latent heat makes accurate temperature control difficult. Rather than attempting to correct for this effect, we simply discarded data obtained at temperatures where significant freezing effects were detected. At low temperatures, where the sample temperature is the principal source of error, the experimental uncertainty in R_1 was estimated by propagating a 0.1 K temperature error using the known temperature dependence of R_1 for bulk water. At 238 K, for example, this yields an R_1 uncertainty of 1.3%, in good agreement with reproducibility tests at this temperature.

Analysis of ^{17}O Magnetic Relaxation Data. The water ^{17}O longitudinal relaxation rate, R_1, selectively monitors the rotational dynamics of water molecules. For a dilute solution of a protein containing N_I internal water molecules with residence time $\tau_I \ll 1\ \mu s$[26,27,29]

$$R_1(\omega_0) = \left(1 + \frac{\nu_{dyn}}{N_W}\right)R_1^0 + \frac{N_I S_I^2}{N_W}\frac{\omega_Q^2}{5}\left[\frac{\tau_c}{1 + (\omega_0\tau_c)^2} + \frac{4\tau_c}{1 + (2\omega_0\tau_c)^2}\right] \quad (1)$$

where N_W is the known water/protein mole ratio; R_1^0 is the relaxation rate measured in a separate protein-free reference sample; ω_0 is the ^{17}O resonance frequency; and $\omega_Q = 7.61 \times 10^6\ s^{-1}$ is the ^{17}O nuclear quadrupole frequency in an immobilized water molecule.[26]

The first term in eq 1 contains the contributions from water molecules in the bulk solvent (unaffected by the protein) and in the hydration layer, characterized by the dynamic hydration number

$$\nu_{dyn} = N_H(\xi - 1) \quad (2)$$

where N_H is the number of water molecules in the layer and ξ is their average dynamic perturbation factor (DPF), defined as the average rotational correlation time of the N_H hydration water molecules divided by the same quantity for bulk water (in the reference sample).

The second term in eq 1 is the contribution from the N_I internal water molecules with mean-square orientational order parameter S_I^2 and correlation time τ_c. The latter is determined by the rotational correlation of the protein, τ_P, and the mean residence time, τ_I, of the internal water molecules according to

$$\tau_c = \left(\frac{1}{\tau_P} + \frac{1}{\tau_I}\right)^{-1} \quad (3)$$

The temperature dependence of the DPF was modeled by assuming a power-law distribution for the rotational correlation time, τ_H, of the N_H hydration water molecules, $f(\tau_H) \propto \tau_H^{-\nu}$, as suggested by molecular dynamics simulations.[37,38] In this model,[29] the DPF is determined by two parameters: the power-law exponent, ν, and the activation energy, E_H^-, for rotation of the most mobile water molecules in the hydration layer. The DPF depends weakly on frequency at low temperatures because τ_H for the slowest hydration waters is then comparable to $1/\omega_0$. The quantity $\xi(\omega_0)$ derived by means of eqs 1 and 2 is therefore an apparent DPF, which, in general, is slightly smaller than the true DPF, $\xi = \langle\tau_H\rangle/\tau_{bulk}$. For simplicity, the minor difference between the apparent and true DPFs will be disregarded in the following, although it was fully included in the quantitative data analysis.

RESULTS AND DISCUSSION

Assessment of Protein Structure. Far-UV circular dichroism (CD) and high-resolution ^1H NMR spectra were recorded at 300 K to assess the structure of wild-type protein L (ProtL) and the Kx6E mutant under our solution conditions. Both proteins were studied without added salt (except for buffer), and the Kx6E mutant was also studied in the presence of 750 mM NaCl. On the basis of previous NMR studies,[7] we expect the mutant to be largely unfolded in the absence of salt and largely folded in 750 mM NaCl. The CD spectra for ProtL and Kx6E with salt are virtually identical (Figure 1), indicating,

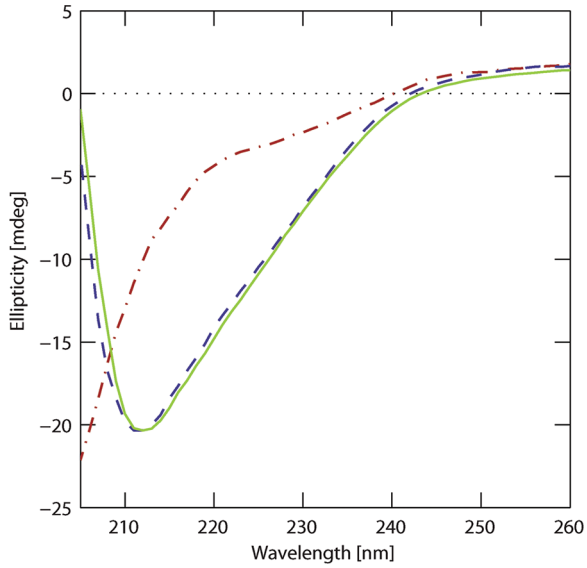

Figure 1. Circular dichroism spectra at 300 K from ProtL (green solid curve), Kx6E with salt (blue dashed curve), and Kx6E without salt (red dash-dot curve). The spectra have been intensity normalized.

as expected,[7] that both proteins are predominantly folded. In contrast, the CD spectrum for Kx6E without salt indicates extensive loss of secondary structure, as expected if the highly charged protein is largely unfolded.

To further assess the structure of the mutant, we recorded ^1H NMR spectra at 600 MHz for Kx6E with and without salt (Figure 2). In the presence of salt, the peaks are well dispersed in both amide and methyl (not shown) regions, as expected for a well-folded protein. In the absence of salt, the spectrum collapses partly, as expected for an unfolded protein. The remaining chemical shift dispersion in the backbone amide

dx.doi.org/10.1021/jp3000569 | J. Phys. Chem. B 2012, 116, 3436−3444

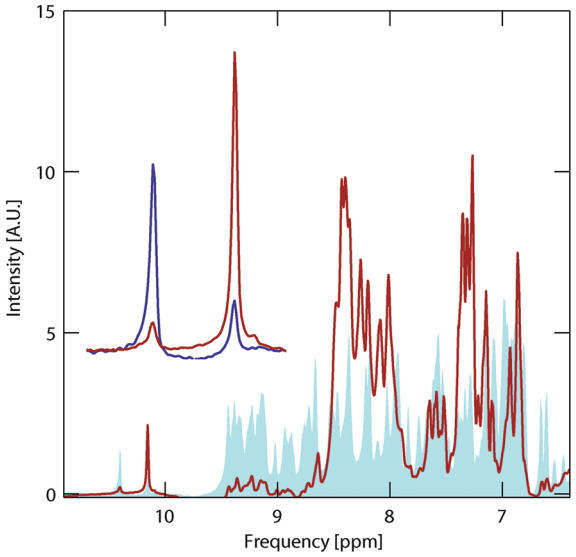

Figure 2. Amide region of 600 MHz ^{1}H NMR spectra at 300 K from Kx6E with salt (blue curve and light blue area) and without salt (red curve). The inset magnifies the Trp-47 side-chain HN peak near 10.2 (unfolded) or 10.4 (folded) ppm.

region is similar to that reported for a mutant of ProtL denatured by guanidinium chloride, where the chemical shifts were close to the random-coil limit and only a small amount of secondary structure could be detected.[23]

For a more quantitative assessment of the degree of unfolding, we used the integrated intensity of the Trp-47 side-chain HN peak (Figure 2, inset). We thus estimate that the sample without salt contains ∼9% folded protein, while the sample with salt contains ∼16% unfolded protein.

Protein and Internal Water Dynamics. The water ^{17}O longitudinal relaxation rate, R_1, exhibits a dispersion in the megahertz frequency range only if the protein contains one or more water molecules with mean residence time, τ_I, in the nanosecond−microsecond range.[26,27] This dispersion is described by the second term of eq 1. Such long-lived water molecules are invariably buried in deep pockets or cavities within the native protein structure. Unfolded proteins lacking disulfide bonds (ProtL has no cysteine) are not expected to give rise to a ^{17}O relaxation dispersion since they lack the persistent structure required to trap water molecules for times longer than ∼1 ns.[28]

Figure 3 shows the ^{17}O magnetic relaxation dispersion (MRD) profiles recorded at 300 K from solutions of ProtL and the mutant Kx6E with and without salt. The protein concentration in the three samples was different (Table 1), but the data shown in Figure 3 have been normalized to the concentration of the ProtL sample using the fact that the protein-induced relaxation enhancement, $R_1 - R_1^0$, is inversely proportional to the known water/protein mole ratio, N_W, as seen from eq 1.

The MRD profiles from ProtL and (folded) Kx6E with salt are well described by eq 1 with the values of the three adjustable parameters given in Table 1. The values 0.7 ± 0.1 (ProtL) and 0.8 ± 0.2 (Kx6E) obtained for $N_I S_I^2$, the product of the number of long-lived internal water molecules (N_I), and their mean-square order parameter ($S_I^2 \leq 1$) demonstrate that both proteins contain (at least) one long-lived water molecule. The 1.7 Å crystal structure[21] 1HZ6 of ProtL reveals no fully buried water molecule, but two water molecules reside in deep

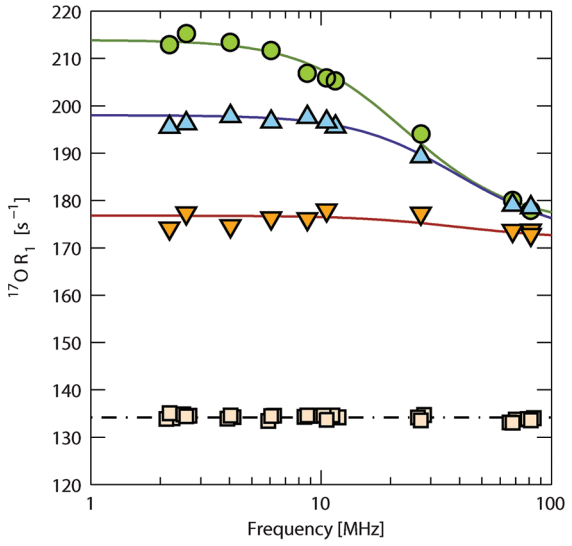

Figure 3. Frequency dependence of the water ^{17}O longitudinal relaxation rate, R_1, at 300 K from ProtL (green circles) and Kx6E with salt (blue triangles) and without salt (orange inverted triangles). The relaxation rates, R_1^0, from the three different reference samples (squares) are slightly displaced in frequency for visual clarity. The curves resulted from fits according to eq 1 with the parameter values given in Table 1. The relaxation rate from the protein solutions has been scaled to the concentration of the ProtL sample. For Kx6E with salt and the corresponding salt-containing reference sample, the small frequency-independent salt-induced R_1 enhancement (4.0 s^{-1}) has been subtracted.

Table 1. Sample Characteristics and Results Derived from ^{17}O MRD Data at 300 K

property	ProtL	Kx6E with salt	Kx6E without salt
C_P (mM)	12.4	8.2	7.4
N_W	4005	6332	7042
ν_{dyn}	1216 ± 30	1102 ± 82	1138 ± 31
$N_I S_I^2$	0.70 ± 0.06	0.79 ± 0.23	0.15 ± 0.04
τ_c (ns)	3.83 ± 0.27	2.26 ± 0.47	[2.26]^a
χ^2_{red}	2.07	0.44	0.60

^{a}Frozen during fit.

surface pockets and may therefore[29,39,40] have residence times in the nanosecond range, as required to account for the observed ^{17}O dispersions. These water molecules are secluded (limited solvent exposure), and both of them make two strong hydrogen bonds to the protein, as detailed in the Supporting Information (Table S1). However, one of these surface pockets is lined by the C-terminal Gly-64 and the loop residues Ala-13 and Asn-14, which may be disordered in solution. Indeed, this pocket is devoid of water in one of the three protein molecules in the asymmetric unit.[21] It is therefore likely that the ^{17}O dispersions are produced by the single water molecule shown in Figure 4. We cannot exclude the possibility that both water molecules contribute, but their mean square order parameter would then have to be as low as 0.35−0.40.

The correlation time, τ_c = 3.8 ± 0.3 ns, deduced from the ProtL MRD profile matches the rotational correlation of the protein, τ_P = 3.9 ns, obtained from molecular hydrodynamics calculations[41] based on the crystal structure 1HZ6[21] with an atomic element radius of 3.0 Å.[42] In view of eq 3, this finding implies that the residence time, τ_I, of the internal water molecule in ProtL is much longer than 4 ns. Conversely, the

dx.doi.org/10.1021/jp3000569 | J. Phys. Chem. B 2012, 116, 3436−3444

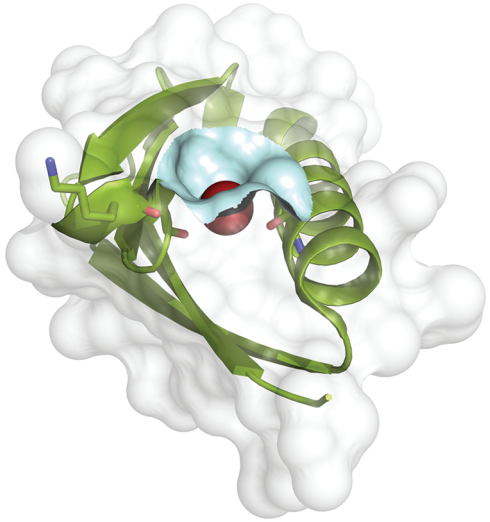

Figure 4. Putative long-lived water molecule (red sphere) residing in a surface pocket (cyan surface) of ProtL (green cartoon, white transparent surface). Shown in stick representation are the two residues (Thr-30 and Gly-55) that are H-bonded to this water molecule and a nearby residue, Lys-54, which is mutated in Kx6E. Rendered using PyMol 1.4 and standard unified vdW radii.

shorter correlation time, τ_c = 2.3 ± 0.5 ns, deduced for Kx6E implies that the residence time of the internal water molecule is shortened by the mutations. With τ_P = 3.9 ± 0.4 ns, eq 3 yields τ_I = 5.4 ± 3.0 ns. This shortening of the residence time is plausible since one of the substituted residues, Lys-54, is close to the probable location of the internal water molecule (Figure 4). This mutation-induced reduction of the internal water residence time is the reason for the smaller amplitude of the ^{17}O dispersion step for Kx6E as compared to ProtL (Figure 3).

For Kx6E without salt, the ^{17}O dispersion is barely significant (Figure 3). Since the dispersion amplitude is comparable to the experimental error in R_1, the two parameters $N_IS_I^2$ and τ_c cannot be determined simultaneously. The ^{1}H NMR spectra indicate that a minor fraction of the protein remains folded in the absence of salt (Figure 2), so we expect a small dispersion from this fraction. Consequently, we fit the ^{17}O dispersion for Kx6E without salt with the correlation time frozen to 2.26 ns (as for Kx6E with salt). The resulting parameter value $N_IS_I^2$ = 0.15 ± 0.04 should then be interpreted as the product of $N_IS_I^2$ for the folded protein and the fraction of folded protein. We thus infer that 19 ± 8% of the protein is folded, not far from the (equally crude) estimate (9%) based on the ^{1}H NMR spectrum. Since the small dispersion can be explained by a minor fraction of folded protein, we conclude that the water molecules interacting with the unfolded protein are mobile, with subnanosecond correlation times. (Water molecules with correlation times of 1 ns and longer would produce a dispersion in the examined frequency window.)

Hydration Dynamics of a Halophilic Protein. The third parameter obtained from the ^{17}O MRD fits in Figure 3 is the dynamic hydration number, $\nu_{dyn} = N_H(\xi - 1)$, involving the number of water molecules in the hydration layer, N_H, and the dynamic perturbation factor (DPF), ξ, which is the rotational correlation time averaged over all N_H water molecules in the hydration layer divided by the water rotational correlation time in the bulk solvent.

The hydration number, N_H, was estimated by dividing the solvent-accessible surface area, A_{SA}, by the average solvent-accessible surface area, 10.75 Å^2, occupied by one water molecule, as inferred from molecular dynamics simulations.[29,43] For the folded proteins, A_{SA} was computed with the program[44] GetArea, using a probe radius[29,43] of 1.7 Å, the default set of van der Waals radii,[45] and the (first model of the) solution structures 2PTL[20] (residues 15−78) for ProtL and 2KAC for Kx6E.[7] The resulting N_H values (Table 2) were then combined with the experimentally derived ν_{dyn} values (Table 1) to obtain ξ = 4.0 ± 0.1 for ProtL and 3.6 ± 0.2 for Kx6E.

Table 2. Results Derived from the Temperature Dependence of ν_{dyn}

property	ProtL	Kx6E with salt	Kx6E without salt
N_H[a]	405	421	972
ν	2.23 ± 0.01	2.27 ± 0.01	2.80 ± 0.03
E_H^- (kJ mol^{-1})	27.0 ± 0.3	27.0 ± 0.3	25.6 ± 0.4
χ^2_{red}	1.32	0.56	3.50

[a]Estimated from the solvent-accessible surface area.

From previous ^{17}O MRD studies of 11 monomeric proteins, ξ = 4.2 ± 0.4 (mean ± standard deviation).[39] Wild-type ProtL is thus a typical protein with regard to hydration dynamics, whereas the Kx6E mutant has a slightly more mobile hydration layer. (Only a minor part of the 10% reduction in $\xi = \langle\tau_H\rangle/\tau_{bulk}$ for Kx6E can be explained by the 3% salt-induced increase of τ_{bulk} in the 750 mM NaCl solvent, as inferred from R_1^0 for the bulk solvent reference samples.) Clearly, the large number of carboxylate groups and the large negative net charge density on the surface of Kx6E do not slow down water dynamics, as one might expect for a "highly ordered, multilayered solvation shell"[16] of "immobile" and "tightly bound water molecules".[4,15] We note that the DPF reported here is deduced under the well-founded[29,39] assumption that the effect of the protein on water dynamics is essentially confined to the first layer of (N_H) water molecules covering the protein surface. If the perturbation had a longer range, so that more water molecules were affected, then the dynamic hydration number obtained from the ^{17}O MRD data would yield an even smaller average DPF.

To probe the hydration dynamics in more detail, we investigated the temperature dependence of the dynamic hydration number. This was done by measuring R_1 at a high frequency (81.3 MHz) and subtracting off the small internal-water contribution with the aid of eq 1 and the parameter values in Table 1. (At this high frequency, the internal-water correction is small at room temperature and negligible at the lower temperatures.) Denoting the corrected R_1 value by R_1', we then obtained the dynamic hydration number from eq 1 as $\nu_{dyn} = N_W(R_1'/R_1^0 - 1)$. The results are shown in Figure 5.

The temperature dependence of $\nu_{dyn}(T)$ was analyzed with a model that describes the broad distribution of correlation times, τ_H, in the heterogeneous hydration layer with a power-law exponent ν.[29] A maximum in $\nu_{dyn}(T)$ is observed for all three samples (Figure 5). Neglecting any temperature dependence in N_H, the maximum occurs at the temperature where the activation energy for water rotation is the same in the hydration layer as in the bulk solvent.[29] At temperatures below the maximum, hydration water thus rotates with *lower* activation energy than in the bulk solvent and vice versa.

For the folded proteins, the temperature dependence of $\nu_{dyn}(T)$ is well described by the model (Figure 5). The parameter values resulting from the fits (Table 2) are nearly the same for the two proteins, and they are also very close to the

dx.doi.org/10.1021/jp3000569 | J. Phys. Chem. B 2012, 116, 3436−3444

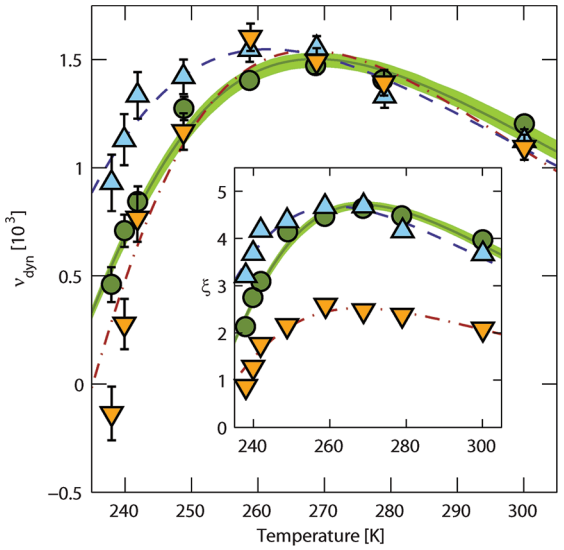

Figure 5. Temperature dependence of the dynamic hydration number, ν_{dyn}, for ProtL (green circles) and Kx6E with salt (blue triangles) and without salt (orange inverted triangles). The curves are model fits to the three data sets (green solid, blue dash, and brown dash-dot, respectively) with the parameter values given in Table 2. For ProtL, the 95% confidence interval of fit is also shown (light green area). The inset shows the DPF, ξ, derived from ν_{dyn} with N_H estimated from the solvent-accessible surface area.

values found previously for the similarly sized proteins BPTI and ubiquitin.[29] This finding implies that, in the examined 60 K temperature range, the average rotational correlation time, $\langle\tau_H\rangle$, of water molecules interacting with the highly charged surface of the halophilic protein Kx6E is indistinguishable from that of nonhalophilic proteins. In other words, there is no discernible halophilic signature in the hydration dynamics, as would be expected if halophilic proteins were more strongly or extensively hydrated.[4,15,16] It should be noted that the difference in ν_{dyn} at low temperatures between ProtL and folded Kx6E (Figure 5) is mainly a consequence of the weaker temperature dependence of the *bulk* water relaxation rate, R_1^0, in the presence of 750 mM NaCl. If we consider instead the quantity $N_W(R_1 - R_1^0) = \nu_{dyn}R_1^0$, the difference between the two proteins almost disappears, as shown in Supporting Information, Figure S1.

The finding that the replacement of six lysines with glutamates has little or no effect on the global hydration dynamics is consistent with the conclusion from previous ^{17}O MRD studies of numerous proteins that ν_{dyn} is not significantly correlated with the net protein charge, the total number of charged residues, the total number of carboxylate groups, or with any of these quantities normalized by the solvent-accessible surface area of the protein.[39] By recording ^{17}O MRD profiles for ubiquitin as a function of pH, a small increase in ν_{dyn} was observed upon deprotonation of the 12 carboxyl groups at 300 K.[46] For the proteins examined here, this result translates into a 10% increase in ν_{dyn} on introducing six glutamate residues. We find that these mutations result in a 9 ± 7% *decrease* in ν_{dyn} at 300 K (Table 1), but this can be explained by the loss of 6 × (4 − 2) = 12 methylene groups, which are known to slow down water dynamics significantly,[40,43,47] when six lysines are replaced by glutamates. All results from the present and previous water ^{17}O relaxation studies are consistent with the picture emerging from molecular dynamics simulations,[38,48−50] where protein hydration dynamics are governed chiefly by surface topography rather than by the chemical structure, charge, or polarity of the hydrated residues.

Hydration Dynamics of an Unfolded Protein. We now focus on the unfolded Kx6E mutant (without salt) to elucidate what the ν_{dyn} data tell us about the hydration of the ensemble of unfolded polypeptide conformations. Since very little is known about the statistical structure (and any residual native-like structure) of unfolded proteins, the hydration number, N_H, cannot be estimated as reliably as for folded proteins. We expect N_H to increase substantially upon unfolding, but the ν_{dyn} parameter deduced from the ^{17}O MRD profiles from Kx6E (at 300 K) increases by merely 3% upon unfolding (Table 1). In view of eq 2, this finding suggests that the expected increase in N_H is nearly compensated by a decrease in the DPF, ξ, as previously inferred for acid-denatured apomyoglobin.[28,34]

For folded proteins, the DPF is dominated by a minor fraction of the ∼400 water molecules in the hydration layer.[29,39] These more strongly perturbed water molecules, which are thought to reside in concave regions (pockets) on the surface,[38,48−50] are responsible for the long-τ_H tail of the power-law distribution in our model (see Materials and Methods). When the protein unfolds, these special hydration sites are destroyed with a consequent large reduction of the DPF. On the other hand, if the unfolded protein is relatively compact, the occluded water molecules may be more dynamically perturbed than most water molecules in the hydration layer of the folded protein, leading to an increased DPF. Such a scenario was invoked to explain the large DPF increase found for protein unfolding induced by urea[35] or guanidinium chloride.[34] The DPF reduction found on unfolding of Kx6E suggests a more expanded denatured state, where dynamic occlusion effects are unimportant. This picture is consistent with the high net charge (−15) of the Kx6E mutant and the lack of disulfide bonds, factors that favor expanded polypeptide conformations.

Turning now to the temperature dependence of ν_{dyn} for unfolded Kx6E (Figure 5), we note that ν_{dyn} is negative at 238 K. This means that, at this temperature, the water molecules that interact with the unfolded protein rotate *faster* on average than in bulk water. In general, the experimental data cannot yield N_H and ξ separately but can only provide the combination $N_H(\xi - 1) = \nu_{dyn}$. However, at the temperature where $\nu_{dyn} = 0$, we can, without knowing N_H, conclude that the mean rotational correlation time, $\langle\tau_H\rangle$, in the hydration layer is equal to the rotational correlation time, τ_{bulk}, in the bulk solvent ($\xi = 1$). In previous studies of folded proteins,[29,35] this zero-crossing could not be observed since it occurs at temperatures below the practical limit of supercooling.

As noted above, ν_{dyn} for folded Kx6E is larger than for ProtL at low temperatures mainly because water rotates faster in bulk 750 mM NaCl than in pure water at these temperatures. (The opposite is true at room temperature.) To avoid this complication, we shall compare ν_{dyn} for unfolded Kx6E with ν_{dyn} for folded ProtL, both without salt. At the zero-crossing temperature of ∼238 K, we know that $\xi = 1$ for unfolded Kx6E. At this temperature, the ν_{dyn} value in Figure 5 yields, with N_H = 405 (Table 2), $\xi \approx 2$ for folded ProtL. Without any assumptions about the structure of the unfolded protein, we can thus conclude that, at 238 K, the water molecules interacting with unfolded Kx6E rotate on average twice as fast as the water molecules in the hydration layer of folded ProtL.

dx.doi.org/10.1021/jp3000569 | J. Phys. Chem. B 2012, 116, 3436−3444

To fit the power-law model to the temperature dependence of ν_{dyn}, we need to estimate N_H for unfolded Kx6E. Several methods have been proposed for computing the solvent-accessible surface area, A_{SA}, of unfolded proteins by generating ensembles of disordered polypeptide chains (or fragments thereof) with the aid of empirically or theoretically based conformational libraries.[51−53] However, none of these methods treat the polypeptide−water interaction explicitly. Using one of these methods,[54] we find that A_{SA} for Kx6E increases by 61% upon unfolding. The area per water molecule, A_{SA}/N_H, is not necessarily the same for unfolded and folded proteins. For example, two polypeptide segments may have a shared hydration shell. However, by using a probe radius of 2.8 Å (rather than the standard 1.4 Å), we find[54] a somewhat *larger* increase (72%) in A_{SA} upon unfolding of Kx6E, suggesting that the conformations sampled with this method are not compact.

The power-law model cannot fully reproduce the observed temperature dependence in ν_{dyn} for unfolded Kx6E for any parameter values (Figure 5). To produce a sharper maximum in $\nu_{dyn}(T)$, as observed for unfolded Kx6E, the model requires substantially larger values for N_H and for the power-law exponent, ν. Using a value of N_H that is 61% larger than for folded Kx6E (see above), we obtain a poor fit ($\chi^2_{red} \approx 6$) with a larger exponent, $\nu = 2.5$, than for the folded proteins (Table 2). With N_H 3−4 times larger than for the folded protein, which is unphysical, we obtain a somewhat better fit ($\chi^2_{red} \approx 2.7$) with a large exponent ($\nu \approx 3.2$). The fit shown in Figure 5 refers to an intermediate case, with N_H 2.4 times larger than for folded Kx6E, yielding $\nu = 2.8$.

The wide range of correlation times, τ_H, in the hydration layer of folded proteins (from a few picoseconds to 1 ns at room temperature), which we model with a power-law distribution, is a consequence of the convoluted surface topography of folded proteins.[29,39] For an unfolded protein that samples an ensemble of noncompact conformations, we expect a more narrow distribution of correlation times. In particular, the long-τ_H tail associated with secluded hydration sites should be absent. We believe that this is the main reason for the failure of the power-law model to describe $\nu_{dyn}(T)$ for unfolded Kx6E. A more narrow distribution is also consistent with the larger exponents derived from the model fits.

CONCLUDING REMARKS

It is widely believed that halophilic proteins are protected against unfolding and aggregation at high salinity by an exceptional hydration induced by their high surface density of negatively charged carboxylate groups.[3,4,10−16] Here, we have tested this hypothesis by directly and specifically monitoring the rotational dynamics of water molecules interacting with the surfaces of the halophilic model protein Kx6E and its mesophilic counterpart ProtL. We find that the halophilic protein is indistinguishable from ProtL and other, previously studied,[29] nonhalophilic proteins with regard to hydration dynamics. This is the case at room temperature and all the way down to the practical limit of supercooling (238 K), where any differences might have been amplified. These results are consistent with the previously noted lack of correlation between hydration dynamics and protein surface charge density.[39] Since Kx6E is structurally and thermodynamically similar to naturally occurring halophilic proteins, the lack of halophilic signature in the hydration dynamics of this protein challenges the widely held belief that halophilic proteins perturb the surrounding water more extensively than non-halophilic proteins. Although there is no causal link between thermodynamics and kinetics, an unusual hydration structure, had it existed, would have affected both protein stability and hydration dynamics. The absence of a correlation between the latter two properties thus argues against an unusual hydration structure for halophilic proteins.

The arguments used to support this notion tend to invoke the concept of "bound" water, which is usually defined operationally without specifying how and to what extent the physical properties, such as H-bond coordination or molecular mobility, differ from those of bulk water. Crystallographers often refer to well-resolved peaks in the solvent electron density as "bound" or even "tightly bound" water. Such peaks reveal spatial correlations between water oxygens and protein atoms, but they have no kinetic or energetic implications. Indeed, the water is usually in a vitreous immobile state when X-ray diffraction data are recorded, whereas ^{17}O relaxation[29,39] and computer simulations[38,48−50] of protein solutions show that the corresponding water molecules move on a picosecond time scale at room temperature.

Another operational definition uses the term "bound" to describe the water molecules that are not incorporated into the ice lattice when a protein solution is kept at 238 K.[17,55] Antifreeze proteins have binding surfaces that match the periodicity of the ice crystal,[56] but other proteins are not expected to bind directly to ice.[57] It is therefore not surprising that a small number of water molecules (less than half a monolayer for hen lysozyme[17,55]) remain in a disordered mobile state between the protein and ice surfaces. The finding that more unfrozen water is found at 238 K near charged amino acid side chains leads to the prediction that "the hydration of proteins should be quite sensitive to acid titration".[17] This may be true if "bound" water is defined as unfrozen water at 238 K, but the present work and previous ^{17}O relaxation studies[29,39,46] and computer simulations[38,48−50] show that it is not true for the water molecules interacting with proteins in aqueous solution, either at 238 K or at room temperature.

The 250-fold mobility reduction for cell water in the extreme halophile *H. marismortui*, inferred from quasielastic neutron scattering (QENS) data, was linked to anomalous hydration of halophilic proteins and was taken to indicate "a specific water structure responsible for the large amount of K^+ bound within these extremophile cells",[18] a viewpoint[58] that was hotly debated before the discovery of ion pumps. In contrast, ^2H MRD measurements show the same modest (factor 3−4) cell-averaged mobility reduction in *H. marismortui* as in *E. coli*.[59] It was concluded[59] that the MRD result is consistent with the current picture of hydration dynamics for nonhalophilic proteins, and we can now state that this applies also for halophilic proteins. In an attempt to reconcile the divergent QENS and MRD results for *H. marismortui*, it was suggested that the water molecules interacting with halophilic proteins "would find their translational diffusion inhibited, with only slightly affected reorientational motions".[19] However, the molecules in liquid water invariably translate and rotate on the same time scale since both processes are governed by H-bond rearrangements.[60] In our view, a more likely explanation for the discrepancy between QENS and MRD in this case is the strong model dependence of QENS data interpretation. Indeed, the standard model used to analyze QENS data fails even for bulk water.[61]

Like many other halophilic proteins, Kx6E is unfolded in the absence of salt. This allowed us to study the hydration

dx.doi.org/10.1021/jp3000569 | J. Phys. Chem. B 2012, 116, 3436−3444

dynamics in an unfolded protein without confounding cosolvents or other destabilizing external perturbations. While ^{17}O relaxation data do not in general permit separate determination of the extent of surface hydration (the number, N_H, of perturbed water molecules) and the degree of perturbation (the dynamical perturbation factor, ξ), the finding that, for unfolded Kx6E at 238 K, the relaxation rate, R_1, for the protein solution equals the relaxation rate, R_1^0, for the protein-free solvent allows us to conclude unambiguously (without any model assumptions) that the average rotational correlation time in the hydration layer, $\langle\tau_H\rangle$, equals the rotational correlation time in bulk water, $\tau_{bulk} \approx 35$ ps, at this temperature. For the folded form of the mesophilic analog ProtL, we found a 2-fold larger dynamic perturbation, $\langle\tau_H\rangle \approx 70$ ps, at this temperature.

For the folded forms of Kx6E and ProtL, as for the previously studied proteins BPTI and ubiquitin,[29] the temperature-dependent ^{17}O relaxation data indicate a wide range of water rotational correlation times in the hydration layer that can be described[29] by a power-law distribution, $f(\tau_H) \propto \tau_H^{-\nu}$, with exponent $\nu = 2.2-2.3$. In contrast, the ^{17}O data for unfolded Kx6E indicate a more narrow distribution, lacking the long-τ_H tail associated with the most strongly perturbed water molecules, thought to reside in pockets on the native protein surface. The ^{17}O data are consistent with an expanded structure of the unfolded protein, as expected from its large net charge (−15) and absence of disulfide cross-links. The $f(\tau_H)$ distribution would then be narrow and peaked around the same τ_H value as found for amino acids,[34,47] oligopeptides,[47] and other small organic solutes,[43] 1.5−2.0 times longer than for bulk water at room temperature. A similar picture of an expanded polypeptide chain with weakly perturbed hydration dynamics emerged from a previous ^{17}O MRD study of acid-denatured apomyoglobin (pH 2.2, net charge ∼33, no disulfides),[28,34] whereas proteins denatured by heat,[32] cold,[33] urea,[33,35] or guanidinium chloride[34] appear to be more compact with more strongly perturbed hydration dynamics.

■ ASSOCIATED CONTENT

Supporting Information

H-bond lengths for potentially long-lived water molecules in ProtL (Table S1). ^{17}O relaxation enhancement versus temperature for ProtL and Kx6E (Figure S1). This material is available free of charge via the Internet at http://pubs.acs.org.

■ AUTHOR INFORMATION

Corresponding Author

*E-mail: bertil.halle@bpc.lu.se. Phone: +46 (0)46 222 9516.

Notes

The authors declare no competing financial interest.

■ ACKNOWLEDGMENTS

This work was supported by grants from the Swedish Research Council, the Crafoord Foundation, and the Knut & Alice Wallenberg Foundation (to B.H.) and from the Spanish Ministry of Science and Innovation (to O.M.).

■ REFERENCES

(1) Lanyi, J. K. *Bacteriol. Rev.* **1974**, *38*, 272−290.
(2) Eisenberg, H.; Mevarech, M.; Zaccai, G. *Adv. Protein Chem.* **1992**, *43*, 1−62.
(3) Madern, D.; Ebel, C.; Zaccai, G. *Extremophiles* **2000**, *4*, 91−98.
(4) Mevarech, M.; Frolow, F.; Gloss, L. M. *Biophys. Chem.* **2000**, *86*, 155−164.
(5) Fukuchi, S.; Yoshimune, K.; Wakayama, M.; Moriguchi, M.; Nishikawa, K. *J. Mol. Biol.* **2003**, *327*, 347−357.
(6) Paul, S.; Bag, S. K.; Das, S.; Harvill, E. T.; Dutta, C. *Genome Biol.* **2008**, *9*, R70.
(7) Tadeo, X.; López-Méndez, B.; Trigueros, T.; Laín, A.; Castano, D.; Millet, O. *PLoS Biol.* **2009**, *7*, e1000257.
(8) Elcock, A. H.; McCammon, J. A. *J. Mol. Biol.* **1998**, *280*, 731−748.
(9) Ghosh, T.; Kalra, A.; Garde, S. *J. Phys. Chem. B* **2005**, *109*, 642−651.
(10) Rao, J. K. M.; Argos, P. *Biochemistry* **1981**, *20*, 6536−6543.
(11) Pundak, S.; Eisenberg, H. *Eur. J. Biochem.* **1981**, *118*, 463−470.
(12) Calmettes, P.; Eisenberg, H.; Zaccai, G. *Biophys. Chem.* **1987**, *26*, 279−290.
(13) Zaccai, G.; Cendrin, F.; Haik, Y.; Borochov, N.; Eisenberg, H. *J. Mol. Biol.* **1989**, *208*, 491−500.
(14) Dym, O.; Mevarech, M.; Sussman, J. L. *Science* **1995**, *267*, 1344−1346.
(15) Frolow, F.; Harel, M.; Sussman, J. L.; Mevarech, M.; Shoham, M. *Nat. Struct. Biol.* **1996**, *3*, 452−458.
(16) Britton, K. L.; Baker, P. J.; Fisher, M.; Ruzheinikov, S.; Gilmour, D. J.; Bonete, M. J.; Ferrer, J.; Pire, C.; Esclapez, J.; Rice, D. W. *Proc. Natl. Acad. Sci. U.S.A.* **2006**, *103*, 4846−4851.
(17) Kuntz, I. D. *J. Am. Chem. Soc.* **1971**, *93*, 514−516.
(18) Tehei, M.; Franzetti, B.; Wood, K.; Gabel, F.; Fabiani, E.; Jasnin, M.; Zamponi, M.; Oesterhelt, D.; Zaccai, G.; Ginzburg, M.; Ginzburg, B. Z. *Proc. Natl. Acad. Sci. U.S.A.* **2007**, *104*, 766−771.
(19) Jasnin, M.; Stadtler, A.; Tehei, M.; Zaccai, G. *Phys. Chem. Chem. Phys.* **2010**, *12*, 10154−10160.
(20) Wikström, M.; Drakenberg, T.; Forsén, S.; Sjöbring, U.; Björck, L. *Biochemistry* **1994**, *33*, 14011−14017.
(21) O'Neill, J. W.; Kim, D. E.; Baker, D.; Zhang, K. Y. J. *Acta Cryst. D* **2001**, *57*, 480−487.
(22) Scalley, M. L.; Yi, Q.; Gu, H.; McCormack, A.; Yates, J. R.; Baker, D. *Biochemistry* **1997**, *36*, 3373−3382.
(23) Yi, Q.; Scalley-Kim, M. L.; Alm, E. J.; Baker, D. *J. Mol. Biol.* **2000**, *299*, 1341−1351.
(24) Tadeo, X.; Pons, M.; Millet, O. *Biochemistry* **2007**, *46*, 917−923.
(25) Tadeo, X.; López-Méndez, B.; Castano, D.; Trigueros, T.; Millet, O. *Biophys. J.* **2009**, *97*, 2595−2603.
(26) Halle, B.; Denisov, V. P.; Venu, K. Multinuclear Relaxation Dispersion Studics of Protein Hydration, In *Biological Magnetic Resonance*; Krishna, N. R., Berliner, L. J., Eds.; Kluwer/Plenum: New York, 1999; pp 419−484.
(27) Halle, B.; Denisov, V. P. *Methods Enzymol.* **2001**, *338*, 178−201.
(28) Halle, B.; Denisov, V. P.; Modig, K.; Davidovic, M. In *Protein Folding Handbook*; Buchner, J., Kiefhaber, T., Eds.; Wiley-VCH: Weinheim, 2005; pp 201−246.
(29) Mattea, C.; Qvist, J.; Halle, B. *Biophys. J.* **2008**, *95*, 2951−2963.
(30) Rasmussen, D. H.; MacKenzie, A. P. *J. Chem. Phys.* **1973**, *59*, 5003−5013.
(31) Dill, K. A. *Biochemistry* **1990**, *29*, 7133−7155.
(32) Denisov, V. P.; Halle, B. *Biochemistry* **1998**, *37*, 9595−9604.
(33) Davidovic, M.; Mattea, C.; Qvist, J.; Halle, B. *J. Am. Chem. Soc.* **2009**, *131*, 1025−1036.
(34) Denisov, V. P.; Jönsson, B. H.; Halle, B. *Nat. Struct. Biol.* **1999**, *6*, 253−260.
(35) Modig, K.; Kurian, E.; Prendergast, F. G.; Halle, B. *Protein Sci.* **2003**, *12*, 2768−2781.
(36) Gottschalk, M.; Halle, B. *J. Phys. Chem. B* **2003**, *107*, 7914−7922.
(37) Garcia, A. E.; Hummer, G. *Proteins* **2000**, *38*, 261−272.
(38) Henchman, R. H.; McCammon, J. A. *Protein Sci.* **2002**, *11*, 2080−2090.
(39) Halle, B. *Phil. Trans. R. Soc. London B* **2004**, *359*, 1207−1224.
(40) Halle, B. In *Hydration Processes in Biology*; Bellissent-Funel, M.-C., Ed.; IOS Press: Dordrecht, 1999; pp 233−249.
(41) Ortega, A.; Amorós, D.; García de la Torre, J. *Biophys. J.* **2011**, *101*, 892−898.

(42) Halle, B.; Davidovic, M. *Proc. Natl. Acad. Sci. U.S.A.* **2003**, *100*, 12135−12140.
(43) Qvist, J.; Halle, B. *J. Am. Chem. Soc.* **2008**, *130*, 10345−10353.
(44) Fraczkiewicz, R.; Braun, W. *J. Comput. Chem.* **1998**, *19*, 319−333.
(45) Shrake, A.; Rupley, J. A. *J. Mol. Biol.* **1973**, *79*, 351−371.
(46) Denisov, V. P.; Halle, B. *J. Mol. Biol.* **1995**, *245*, 682−697.
(47) Ishimura, M.; Uedaira, H. *Bull. Chem. Soc. Jpn.* **1990**, *63*, 1−5.
(48) Kovacs, H.; Mark, A. E.; van Gunsteren, W. F. *Proteins* **1997**, *27*, 395−404.
(49) Luise, A.; Falconi, M.; Desideri, A. *Proteins* **2000**, *39*, 56−67.
(50) Makarov, V. A.; Andrews, B. K.; Smith, P. E.; Pettitt, B. M. *Biophys. J.* **2000**, *79*, 2966−2974.
(51) Creamer, T. P.; Srinivasan, R.; Rose, G. D. *Biochemistry* **1997**, *36*, 2832−2835.
(52) Bernadó, P.; Blackledge, M.; Sancho, J. *Biophys. J.* **2006**, *91*, 4536−4543.
(53) Gong, H.; Rose, G. D. *Proc. Natl. Acad. Sci. U.S.A.* **2008**, *105*, 3321−3326.
(54) Estrada, J.; Bernadó, P.; Blackledge, M.; Sancho, J. *BMC Bioinf.* **2009**, *10*, 104.
(55) Kuntz, I. D.; Brassfield, T. S.; Law, G. D.; Purcell, G. V. *Science* **1969**, *163*, 1329−1331.
(56) Garnham, C. P.; Campbell, R. L.; Davies, P. L. *Proc. Natl. Acad. Sci. U.S.A.* **2011**, *108*, 7363−7367.
(57) Siemer, A. B.; Huang, K.-Y.; McDermott, A. E. *Proc. Natl. Acad. Sci. U.S.A.* **2010**, *107*, 17580−17585.
(58) Damadian, R. *Science* **1976**, *193*, 528−530.
(59) Persson, E.; Halle, B. *Proc. Natl. Acad. Sci. U.S.A.* **2008**, *105*, 6266−6271.
(60) Qvist, J.; Persson, E.; Mattea, C.; Halle, B. *Faraday Discuss.* **2009**, *141*, 131−144.
(61) Qvist, J.; Schober, H.; Halle, B. *J. Chem. Phys.* **2011**, *134*, 144508.

Supporting Information

for

Hydration dynamics of a halophilic protein in folded and unfolded states

Johan Qvist, Gabriel Ortega, Xavier Tadeo, Oscar Millet, and Bertil Halle

Table S1. Distances (in Å) between the oxygen of two potentially long-lived water molecules and H-bonding protein atoms in the crystal structure 1HZ6 of ProtL.

Chain	Water #	Thr-30 OG1	Gly-55 O	Water #	Asn-44 O	Ala-13 N
A	67	2.8	2.7	–	–	–
B	74	2.8	2.9	67	2.9	2.9
C	66	3.0	2.9	76	2.9	2.9

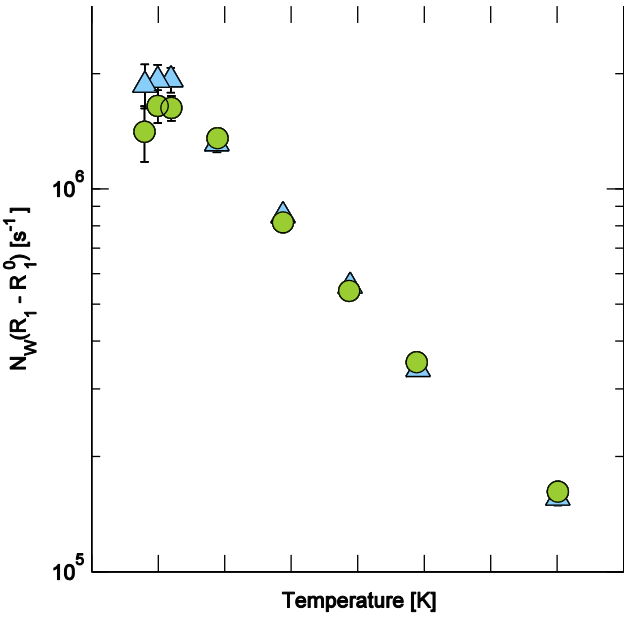

Figure S1. Protein-induced enhancement of the ^{17}O longitudinal relaxation rate at 81.3 MHz, expressed as $N_W(R_1 - R_1^0)$, as a function of temperature for ProtL (green circles) and Kx6E with salt (blue triangles).